JCTC Journal of Chemical Theory and Computation

Article

pubs.acs.org/JCTC

Quantum Corrections to the Free Energy Difference between Peptides and Proteins Conformers

Marco Cecchini*

Laboratoire d'Ingénierie des Fonctions Moléculaires Institut de Science et d'Ingénierie Supramoléculaires, Université de Strasbourg, 8 allée Gaspard Monge, F-67083 Strasbourg Cedex, France

Supporting Information

ABSTRACT: The calculation of the free energy of conformation is key in understanding the function of biomolecules and has attracted significant interest in recent years. Most current computational approaches evaluate the difference in conformational free energy in the classical limit based on the common "dogma" that only the lowest-frequency modes make a significant contribution to it, i.e. they assume that quantum mechanical corrections are negligible. Here, I show for three biomolecular systems described in the rigid-rotor, harmonic-oscillator approximation that the zero-point energy contribution, although small, is not negligible even at room temperature. I find that a quantum correction arises from the intermediate-frequency vibrational modes and that its magnitude is strongly correlated with the number of atoms in the system. A straightforward, though approximate, way to account for this quantum correction in the calculation of conformational free-energy differences by classical molecular dynamics is presented. The relevance of the quantum correction analyzed in this paper is discussed in the context of conventional force fields for proteins.

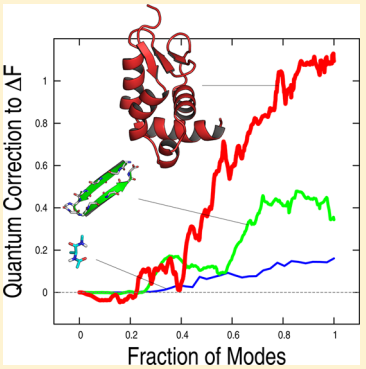

I. INTRODUCTION

Understanding the factors that determine the conformational stability of macromolecules, including e.g. ligand-binding events, requires a thermodynamic analysis. It is well-known, for example, that the small free energy of folding of a protein is a consequence of the cancellation between a large decrease in the enthalpy and a lower decrease in the entropy.[1,2] In principle, given an expression for the potential energy as a function of the atomic coordinates, values of thermodynamic observables such as enthalpy, entropy, and the free energy can be computed from statistical mechanics.[3] In practice, this is a difficult task which suffers from convergence problems in sampling the relevant configurational space, particularly for flexible molecules such as peptides and proteins.[4] As a consequence there exists no generally accepted method for calculating the absolute free energy or the relative free energy for pairs of conformational states of a biomolecule in solution.[5] Classical approaches, such as thermodynamic integration[6] and the exponential formula,[7] have been used for many years in alchemical free-energy difference simulations.[8,9] Recently, refinements with improved force fields and the availability of more computer time have given highly accurate results in some applications.[10,11] However, these methods appear to be unsatisfactory for the study of conformational free energy differences, especially for conformers that differ significantly from each other.[12,13] For this type of problems, more recent developments have shown how to obtain accurate free energy estimates for large conformational changes at a moderate computational cost in a number of applications. They include confinement simulations,[14−19] the "string" free energy method,[20] and nonequilibrium simulations.[21,22]

A limitation of all the approaches above is that they calculate the free energy difference in the classical limit; i.e. quantum mechanical corrections are not included. This is often justified by the argument[23−25] that only the low-frequency modes, which can be approximated classically, make a significant contribution to the differences in thermodynamic quantities for macromolecules (at least at room temperature), such that quantum corrections can be neglected; e.g., approximate quantum calculations of the molecular dynamics have indicated that quantum corrections to the mean-square atomic fluctuations are small above 100 K.[26−28] Now that the computation power is sufficient to perform accurate classical free-energy calculations for cases of interest, it is appropriate to re-examine the question of quantum corrections to the thermodynamics of macromolecules. As an aside, note that for chemical reactions of small molecules and enzymes, particularly for cases involving hydrogen transfer, quantum corrections including those arising from zero-point energy and tunneling have been shown to be significant at room temperature.[29−32]

As is well-known[3] and was first applied to a protein in 1983,[24] quantum corrections to the thermodynamic quantities (enthalpy, entropy, and free energy) can be calculated straightforwardly in the rigid-rotor, harmonic-oscillator (RRHO) approximation to the molecular mechanics potential surface, which is relatively accurate in the neighborhood of the minimum. Thus, normal-mode[24,25] and quasi-harmonic[23,26,33−35] analyses provide possible, though approximate,

Received: November 10, 2014

DOI: 10.1021/acs.jctc.5b00260
J. Chem. Theory Comput. XXXX, XXX, XXX−XXX

means for determining the quantum correction. These analyses involve a quadratic approximation to the intramolecular potential energy function, which is either imposed by computing the energy second derivatives at the minimum of the potential energy surface (normal-mode approximation) or by obtaining the mean square fluctuations corresponding to an "effective" quadratic potential from a converged molecular dynamics trajectory (quasi-harmonic approximation). The latter involves a much larger computational cost, but it accounts for part of the anharmonicity, which can have a substantial effect on the thermodynamic properties of biomolecules.[33]

In this paper, the harmonic approximation is used to show for several biomolecular systems, i.e. two structured peptides and one subdomain of a large motor protein, that the zero-point energy contribution to the vibrational enthalpy can be significant even for conformational free energy differences at room temperature;[24] the correction is found to be on the order of 1 kcal/mol for the motor domain. By making use of previous calculations based on confinement simulations,[16] the correction was used to obtain quantum-corrected free energy results for the alanine dipeptide and the β-hairpin from protein G in the limit of the harmonic approximation. Note that calculations of quantum corrections to thermodynamic quantities that go beyond the harmonic approximation are possible with path integral methods; see, for example, the use of discretized path integral sampling using a quasi-harmonic reference system.[36,37]

The methods and systems studied are described in the next two sections. The calculated quantum correction in the harmonic approximation and its analysis are presented in the Results section. A discussion of the significance of the results is given in the ending section. To make the paper self-contained and introduce the notation, I briefly summarize the well-known classical and quantum mechanical expressions for the thermodynamics of the systems of interest in the next section.

II. QUANTUM AND CLASSICAL FORMULAS

In what follows, I assume that a molecular mechanics potential, such as that used in the CHARMM program,[38,39] can be used to determine the energy corresponding to the conformational minimum and the molecular vibrations.

a. Quantum Limit. The total free energy in the rigid-rotor, harmonic oscillator (RRHO) approximation[3,25] is

$$F^{QM} = F_{trans} + F_{rot} + F_{vib}^{QM} + U_{ff} \tag{1}$$

where the translational, rotational, and vibrational contributions can be written as

$$F_{trans} = -NkT\left[\frac{3}{2}\ln\left(\frac{2\pi mkT}{h^2}\right) - \ln\frac{N}{V} + 1\right] \tag{2}$$

$$F_{rot} = -NkT\left[\frac{3}{2}\ln\left(\frac{8\pi^2 kT}{h^2}\right) + \frac{1}{2}\ln(\pi I_A I_B I_C) - \ln\sigma\right] \tag{3}$$

and

$$F_{vib}^{QM} = NkT\sum_i^{\kappa}\frac{h\nu_i}{2kT} + \ln(1 - e^{-h\nu_i/kT}) \tag{4}$$

with k the Boltzmann constant, h the Plank constant, m the molecular mass, I_A, I_B, and I_C the principal moments of inertia, σ the symmetry number (which is unity in the present applications), κ the number of internal vibrations, ν_i their frequencies, V the volume of the macroscopic system, and N the number of molecules, which is equal to the Avogadro constant at standard state. The quantity U_{ff} in eq 1 represents the electronic energy of the system at the given minimum calculated with the molecular mechanics force field. In eqs 2−4, semiclassical expressions are used for the translational and rotational contributions, while the vibrational contributions are treated quantum mechanically.

In the context of evaluating changes in free energy between conformers of a biomolecule, it is clear that the translational contribution (eq 2), which depends on the macroscopic volume of the system and the mass of the molecule, cancels out. The rotational contribution (eq 3), which depends on the moments of inertia that may vary upon a change in conformation, is expected to be small. Consequently, the only significant quantum correction may arise from the molecular vibrations, eq 4. The vibrational energy is

$$U_{vib}^{QM} = NkT\sum_i^{\kappa}\left[\frac{h\nu_i}{2kT} + \frac{h\nu_i/kT}{e^{h\nu_i/kT} - 1}\right] \tag{5}$$

and the entropy is

$$S_{vib}^{QM} = Nk\sum_i^{\kappa}\left[\frac{h\nu_i/kT}{e^{h\nu_i/kT} - 1} - \ln(1 - e^{-h\nu_i/kT})\right] \tag{6}$$

In addition, eq 5 can be conveniently decomposed into the zero-point energy

$$Z_{vib}^{QM} = N\sum_i^{\kappa}\frac{h\nu_i}{2} \tag{7}$$

which corresponds to the ground-state temperature-independent energy of the multidimensional quantum harmonic oscillator and the temperature-dependent vibrational energy

$$H_{vib}^{QM} = N\sum_i^{\kappa}\frac{h\nu_i}{e^{h\nu_i/kT} - 1} \tag{8}$$

which arises from the population of the vibrational energy levels at a given temperature (see the SI). Thus, the quantum vibrational free energy in the harmonic oscillator approximation is

$$F_{vib}^{QM} = Z_{vib}^{QM} + H_{vib}^{QM} - TS_{vib}^{QM} \tag{9}$$

Introducing the result of eq 9 into eq 1, the free energy of the macromolecule in a given conformational state can be written as

$$F^{QM}(V, T) = F_{trans} + F_{rot} + Z_{vib}^{QM} + H_{vib}^{QM} - TS_{vib}^{QM} + U_{ff} \tag{10}$$

b. Classical Limit. As the classical approximation is used for the translational and rotational contributions, the only difference in the classical limit arises from the vibrational term, which is

$$F_{vib}^{Cl} = NkT\sum_i^{\kappa}\ln\left(\frac{h\nu_i}{kT}\right) \tag{11}$$

Correspondingly, the classical vibrational energy is

$$U_{vib}^{Cl} = N\sum_i^{\kappa}kT \tag{12}$$

and the entropy is

DOI: 10.1021/acs.jctc.5b00260
J. Chem. Theory Comput. XXXX, XXX, XXX−XXX

$$S_{\mathrm{vib}}^{Cl} = Nk \sum_{i}^{\kappa} \left[1 - \ln\left(\frac{h\nu_i}{kT}\right)\right] \tag{13}$$

so that

$$F^{Cl}(V, T) = F_{\mathrm{trans}} + F_{\mathrm{rot}} + U_{\mathrm{vib}}^{Cl} - TS_{\mathrm{vib}}^{Cl} + U_{\mathrm{ff}} \tag{14}$$

Eqs 10 and 14 show that the vibrational contributions to the system free energy are the only terms that may have significant quantum corrections. Therefore, in the following I restrict the analysis to their contribution to the difference in free energy between conformers of a biomolecule.

III. MOLECULAR SYSTEMS

Three biomolecules of increasing size have been investigated: the alanine dipeptide (12 atoms), the β-hairpin from protein G (160 atoms), and the converter of myosin VI (1442 atoms). These systems were chosen for study to determine how quantum corrections at ambient temperature behave as a function of the size of the molecule and in the presence of external fields that affect the vibrational frequencies, i.e. a restraining potential.

Alanine Dipeptide. The alanine dipeptide is the *N*-acetyl-*N*′-methylamide derivative of alanine and has become a standard model for theoretical studies.[21,40−43] The dipeptide was modeled *in vacuum* with the polar-hydrogen potential function[44] (12 atoms) and infinite cutoffs for the nonbonded interactions. Two conformational states that differ in the dihedral angles of the backbone (ϕ,ψ) were analyzed. They are termed **c7eq** and **c7ax** and correspond to the deepest minima of the potential energy surface *in vacuum*; see Figure 1A. The initial peptide coordinates were taken from a previous study.[16] The conformations were energy minimized by the Adopted Basis Newton−Raphson (ABNR) method until an average rms gradient of 10^{-6} kcal/mol/Å was attained. The resulting structures were used for the calculation of the energy second-derivative (Hessian) eigenvectors and eigenvalues; i.e. the normal-mode analysis. The vibrational frequencies were computed from the Hessian eigenvalues as $\nu_i = 2\pi(\lambda_i)^{1/2}$, with λ_i being the eigenvalue of the *i*-th eigenvector. Six overall translational and rotational modes with frequencies smaller than 0.2 cm^{-1} were found for both conformers. Normal-mode frequencies starting with mode 7 were used to compute the vibrational contributions to the thermodynamic observables in both classical and quantum-mechanical limits.

β-Hairpin from Protein G. The β-hairpin from protein G is a 16-residue peptide known to fold to a β-hairpin structure even in the absence of the rest of the protein.[45] Despite its small size, this peptide has a complex free-energy landscape with several basins (conformational states) separated by high free-energy barriers and has become a model system for folding[46] and the development of methods for the calculation of the free energy of conformation.[16,22] The β-hairpin peptide was modeled with the polar-hydrogen potential energy function in CHARMM[44] with no blocking groups for the terminal residues (160 atoms). Solvation effects were approximated by the EEF1 implicit-solvent model,[47] which contains screened electrostatic interactions and a Gaussian term to represent the hydrophobic interactions; EEF1 is particularly suited for harmonic analyses as is the only implicit solvation model for which analytical second derivatives are available in CHARMM. The *native* β-hairpin (**bhp1**) and the three-stranded β-sheet (**bhp2**) conformers of the 16-residue peptide were analyzed; see Figure 1B. As for the alanine dipeptide, initial coordinates were taken from a previous study.[16] Following the prescriptions above, the two conformers were energy minimized (rms gradient $<10^{-4}$ kcal/mol/Å) and used for the normal-mode analysis. All 474 nonzero frequencies were used for the thermodynamic analysis.

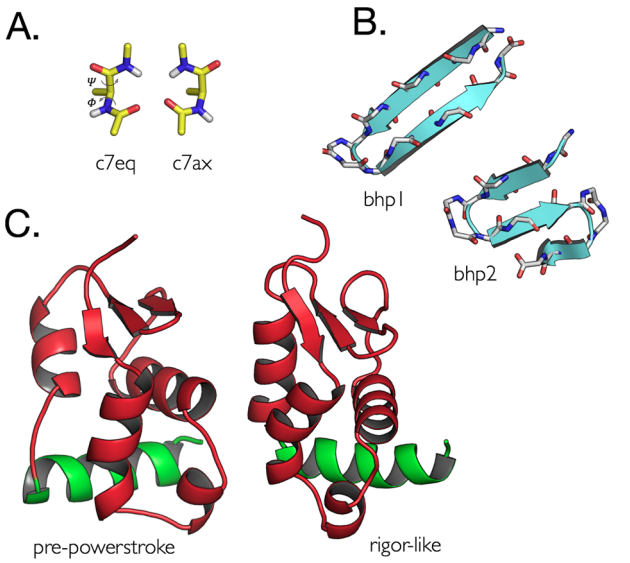

Figure 1. Molecular systems and conformational states used for this study. (A) Alanine dipeptide. The **c7eq** and **c7ax** molecular structures were considered. They correspond to the deepest potential energy minima *in vacuum*. As shown by the arrows, the conformational transition involves a large change of both dihedral angles (ϕ,ψ); **c7eq** (−77.9, 102.6) and **c7ax** (60.7, − 70.3). (B) β-hairpin from protein G. Two molecular states were analyzed: the *native* β-hairpin (**bhp1**) and the three-stranded β-sheet (**bhp2**) conformers. These structures were previously identified as representative of the two deepest free energy basins at 360 K.[46] (C) The converter of the biomolecular motor myosin VI. The converter subdomain and the proximal insert are shown in red and green, respectively. The conformers considered were extracted from the prepowerstroke (PDB: 2V26) and the rigor-like (PDB: 2BKH) X-ray structures of myosin VI. Molecular representations were drawn with the help of PYMOL.[64]

Converter Domain of Myosin VI. The converter is one of the four subdomains making up the head domain of the myosin motor.[48] A recently solved X-ray structure of the prepowerstroke state of myosin VI has revealed a novel fold for the converter,[49] which differs by an RMSD of ∼5 Å from the conventional fold observed in the rigor-like state of myosin VI and all known structures of myosin. As the unconventional fold might explain the exceedingly large step size of myosin VI observed in optical trap experiments,[50] it is of interest to quantify the difference in free energy involved in such a conformational transition.[51] The converter subdomain was modeled with the CHARMM22 force field[52] and the CMAP correction.[53] Solvation effects were approximated by the FACTS implicit-solvent model,[54] which was shown to yield accurate atomic solvation and pair interaction energies when compared with finite-difference Poisson−Boltzmann results. The initial coordinates of the prepowerstroke (**pps**) and the rigor-like (**rig**) conformers of myosin VI were extracted from the corresponding X-ray structures (PDB entries 2V26 and 2BKH, respectively). For this purpose only residues 703−788 were considered, which correspond to the converter subdomain plus the proximal insert; see Figure 1C. The structures of the

DOI: 10.1021/acs.jctc.5b00260
J. Chem. Theory Comput. XXXX, XXX, XXX−XXX

protein were energy minimized using 100 steps of ABNR[39] in the presence of positional harmonic restraints on the protein backbone whose strength was switched from 100 kcal/mol/Å^2 to zero linearly. The resulting structures with the harmonic restraints removed were further optimized by 10000 steps of steepest descent followed by 10000 steps of ABNR (final rms gradient <10^{-4} kcal/mol/Å) previous to the normal-mode analysis. As analytical second derivatives are not available in CHARMM for the FACTS model, an approximate Hessian was computed by the finite difference method. All 4320 nonzero frequencies were used for the thermodynamic analysis.

IV. RESULTS

A. Quantum Correction for the Alanine Dipeptide.

The difference in free energy between the **c7eq** and **c7ax** conformers of the alanine dipeptide *in vacuum* was determined by normal-mode analysis using both quantum and classical formulas; i.e., eqs 10 and 14, respectively. The vibrational frequencies used for the thermodynamic analysis are shown in Figure 2 (circles); their values are given in Table S1. At ambient temperature (300 K) the difference in free energy based on quantum formulas is 2.73 kcal/mol in favor of the **c7eq** conformer; see Table I. As expected the translational contribution is zero and the rotational contribution is small so that ΔF depends only on the vibrational contribution plus the difference in potential energy between the conformers at their minimum (ΔU_{ff}), which is calculated by molecular mechanics. The results in Table I show that the classical and quantum results differ by 0.16 kcal/mol at 300 K, which corresponds to 6% of the total free-energy change in the classical limit. Moreover, as shown by Figure 3 the difference between the classical and quantum results ($\Delta\Delta F$), hereafter referred to as a quantum correction, has contributions from all modes with the largest ones in size arising from the non low-frequency vibrations.

To capture the thermodynamic origin of the quantum correction, both classical and quantum results were separated into components; see eqs 10 and 14. The cumulative trends of the individual contributions to ΔF as a function of the number of modes included in the analysis are shown in Figure 4. In the classical limit (Figure 4, top) the vibrational contribution originates entirely from the entropic term, which converges to 0.5 kcal/mol at mode 17 (~400 cm^{-1}). In this limit, only the low-frequency modes (modes 7−17) contribute to ΔF^{Cl} significantly so that contributions from the higher-frequency vibrations can be safely ignored, as previously recognized.[25] This is not the case in the quantum-mechanical limit. In fact, although the vibrational entropy (ΔS^{QM}_{vib}, eq 6) and the temperature-dependent contribution to the vibrational energy (ΔH^{QM}_{vib}, eq 8) rapidly converge in the low-frequency range (ν < 400 cm^{-1}, modes 7−17), the zero-point energy contribution (ΔZ^{QM}_{vib}, eq 7) does so only at significantly higher frequencies (ν ~ 1600 cm^{-1}, mode 31); see Figure 4 (bottom) and ref 24. In addition, the decomposition shows that ΔS^{QM}_{vib} and ΔZ^{QM}_{vib} are of opposite sign to ΔH^{QM}_{vib}, with the latter favoring the conformer that has the vibrations shifted to higher frequencies; to see this compare the green and the blue circles with the magenta circles in Figure 4 (bottom). Because the contributions introduced by the temperature-dependent vibrational energy (ΔH^{QM}_{vib}) and the zero-point energy term (ΔZ^{QM}_{vib}) nearly cancel out for modes 7−17, the entropic component (ΔS^{QM}_{vib}) predominates in the low-frequency range (ν < 400 cm^{-1}). By contrast, the contributions of the vibrational entropy (ΔS^{QM}_{vib}) and the temperature-

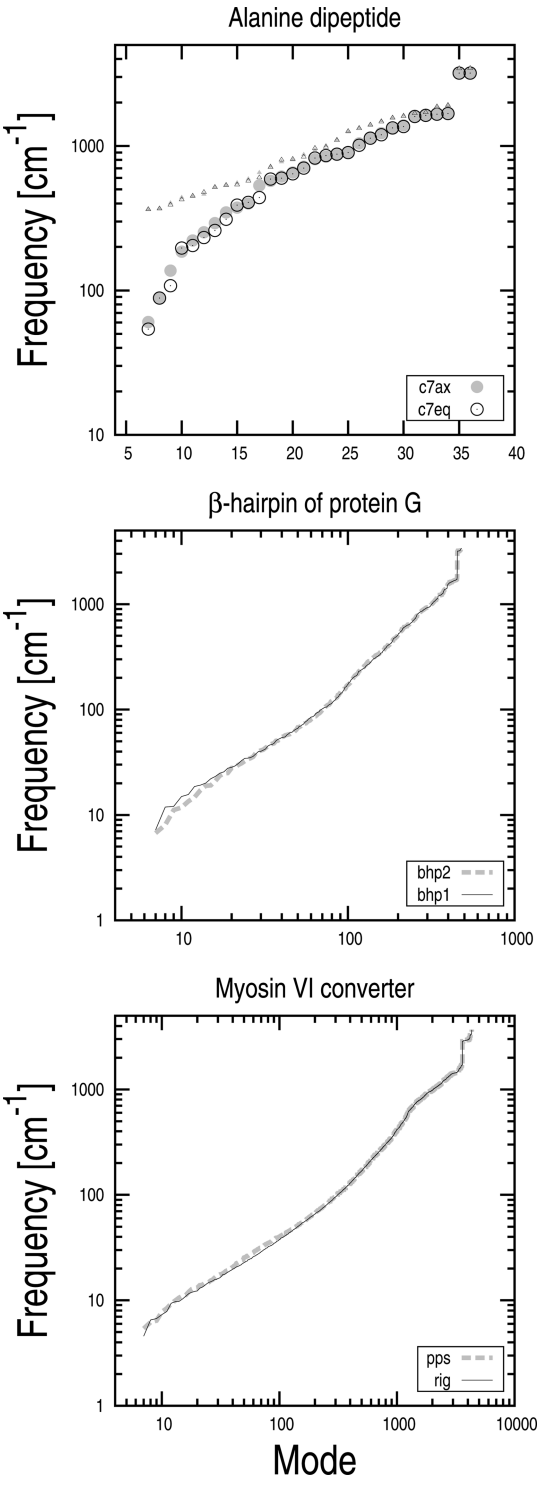

Figure 2. Normal-mode frequencies for conformers of the alanine dipeptide (top), the β-hairpin from protein G (middle), and the converter of myosin VI (bottom). In all cases, the vibrational frequencies of the thermodynamically more stable conformer are shown in black; those of the less stable conformer are shown in gray. On top, the normal-mode frequencies for the alanine dipeptide conformers calculated in the presence of a strong restraining potential (k of 82 kcal/mol/Å^2) are shown as triangles; open and filled triangles correspond to the vibrational frequencies of the **c7eq** and **c7ax** states, respectively. The striking jump observed in the high-frequency range (on the right-hand side) marks the beginning of the vibrational modes involving hydrogen atoms; e.g. NH amide stretching vibrations.

DOI: 10.1021/acs.jctc.5b00260
J. Chem. Theory Comput. XXXX, XXX, XXX−XXX

Table I. Thermodynamic Results for the Three Model Systems Analyzed in the Paper[a]

system	states	ΔF_{trans}	ΔF_{rot}	ΔF^{QM}_{vib}	ΔF^{Cl}_{vib}	ΔU_{ff}	ΔF^{QM}	ΔF^{Cl}	$\Delta\Delta F$
alanine dipeptide	**c7eq/c7ax**	0.0	0.04	0.70	0.54	1.99	2.73	2.57	0.16 (6%)
β-hairpin peptide	**bhp1/bhp2**	0.0	0.12	0.13	−0.21	1.75	2.00	1.66	0.34 (20%)
converter of MyoVI	**rig/pps**	0.0	0.01	5.37	6.46	−0.77	4.61	5.70	1.09 (19%)

[a]All free energy values are given in kcal/mol at 300 K; see Table S3 for the values corresponding to the individual conformers. The translational contribution was evaluated assuming standard conditions, i.e. 1 M concentration. The Δ values correspond to the second conformer minus the first; e.g. for the alanine dipeptide ΔF equals $F_{c7ax} - F_{c7eq}$. The $\Delta\Delta F$ values are defined as $|\Delta F^{QM} - \Delta F^{Cl}|$ and quantify the size of the quantum correction. In parentheses, the correction is given as a percentage of the classical free energy result as $100 \cdot (\Delta F^{QM} - \Delta F^{Cl})/\Delta F^{Cl}$.

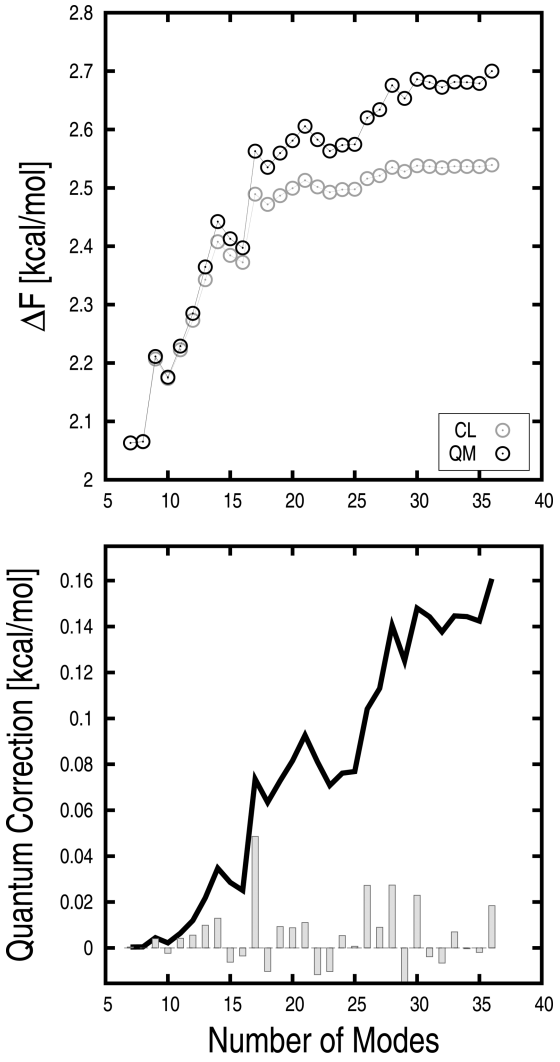

Figure 3. Quantum correction to the difference in conformational free energy between **c7eq** and **c7ax** *in vacuum*. On top, the cumulative trend of the free energy difference as a function of the number of modes included is shown. Modes are sorted by frequency in ascending order. The cumulative ΔF was determined using both quantum (black circles) and classical formulas (gray circles); see eqs 10 and 14. On the bottom, the quantum correction (i.e., the cumulative $\Delta\Delta F$) is shown in black along with contributions from the individual modes as gray bars. The data show that the correction mainly arises from the higher-frequency vibrations (starting at mode 17), which are not well approximated in the classical limit.

dependent vibrational energy (ΔH^{QM}_{vib}) go to zero exponentially with increasing ν, and the zero-point energy is the only frequency-dependent contribution to ΔF in the higher-frequency range (ν > 400 cm^{-1}, modes 18−36); a detailed analysis of the interplay between the vibrational energy and the vibrational entropy contributions in the frequency domain is given in the Appendix and the SI. Thus, the trend of ΔF^{QM} in frequency (Figure 4, black circles) can be effectively deconvoluted into an entropic component, which is dominant in the low-frequency range, and a zero-point energy component that accounts for contributions at higher frequencies. Importantly, the latter can be solely captured by the full quantum mechanical treatment, here in the harmonic approximation. Similar conclusions apply to the β-hairpin peptide and the converter of myosin VI (Figures S3 and S4), which are analyzed below.

The deconvolution of the quantum correction ($\Delta\Delta F$) into its enthalpic and entropic components for the three systems analyzed here shows that the magnitude of the correction is largely dominated by the enthalpic contribution, in particular the zero-point energy difference; see Table S2. The analysis shows that an entropic component, which is significant only for ν > 200 cm^{-1}, is also present but is smaller in size and of opposite sign and effectively reduces the correction by approximately one-third; i.e. $-T\Delta\Delta S/\Delta\Delta U$ in Table S2. The cumulative trends of $\Delta\Delta F$ in the frequency domain (Figure S5) complement these observations and show that the quantum correction arises from the intermediate-frequency vibrations, i.e. 400 < ν < 2000 cm^{-1}. Moreover, as the magnitude of $\Delta\Delta F$ increases "linearly" with the number of modes (Figure 3, bottom), the quantum correction results from individually small but additive contributions of several non low-frequency modes. In addition, the analysis shows that the highest-frequency vibrations, particularly those arising from the NH bonds, do not contribute significantly to the correction despite their inherent quantum character. In fact, as shown by Figure S5, the corrections introduced by these highly localized vibrations, which may be individually large in size, almost cancel out.

Taken together these results indicate that the zero-point energy contribution is primarily responsible for the quantum correction analyzed in this paper. The correction arises mainly from groups or bands of vibrational modes in the intermediate-frequency range, which describe delocalized vibrations that are affected by the conformation of the biomolecule, i.e. the spatial arrangement of atoms.

B. Size Dependence of the Quantum Correction. The magnitude of the correction presented above was analyzed as a function of system size. As the correction originates mainly from the non low-frequency modes, its magnitude is expected to increase with the size of the protein. To verify this hypothesis, the difference in free energy between pairs of conformers of the β-hairpin of protein G (160 atoms) and the converter of myosin VI (1442 atoms) were determined by normal-mode analysis using both quantum and classical formulas; the results are given in Table I. As for the alanine dipeptide, the largest contributions to ΔF arise from the

DOI: 10.1021/acs.jctc.5b00260
J. Chem. Theory Comput. XXXX, XXX, XXX−XXX

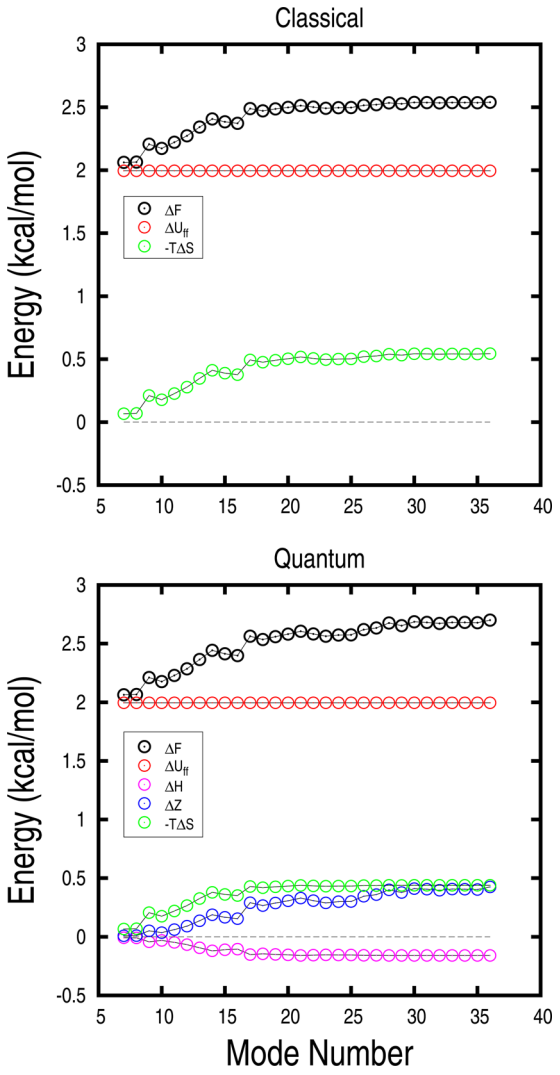

Figure 4. Decomposition of ΔF between the **c7eq** and **c7ax** conformers of the alanine dipeptide. Cumulative trends as a function of the number of modes included are shown for each component. Modes are sorted by frequency in ascending order. On top, the decomposition is performed in the classical limit. Here, the difference in conformational free energy (black) is given by the sum of a constant enthalpic term (red) coming from the molecular mechanics energies at the minimum and an entropic term (green) that depends on the vibrational frequencies of the two conformers; see eq 7 in the SI. On the bottom, the decomposition is done in the quantum-mechanical limit. Here, the enthalpic contribution to ΔF includes two additional frequency-dependent terms: the zero-point energy difference (blue) and the temperature-dependent vibrational energy change (magenta). In the low-frequency range (ν < 400 cm^{-1}), these two contributions cancel out and the vibrational contribution to the difference in conformational free energy varies as the vibrational entropy change (green). In the higher-frequency range (ν > 400 cm^{-1}), both the vibrational entropy and the temperature-dependent vibrational energy contributions go to zero, and the zero-point energy difference (blue), which is temperature independent, is the only term contributing to the difference in conformational free energy; see the Appendix.

vibrational term and the molecular mechanics energy at the minimum. In the case of the β-hairpin, the vibrational contribution is small (less than 0.2 kcal/mol), and the molecular mechanics energy difference (1.75 kcal/mol) is dominant. However, because the quantum and classical results for the vibrational free-energy change (ΔF_{vib}) have opposite signs (see Table I), the quantum correction is still large, i.e. 20% of the classical free energy result. For the converter of myosin, the vibrational term is largely dominant, but the size of the correction is still about 20% of the classical ΔF.

The cumulative trend of the quantum corrections versus the fraction of modes included in the analysis for the three biomolecular systems is compared in Figure 5. The results show

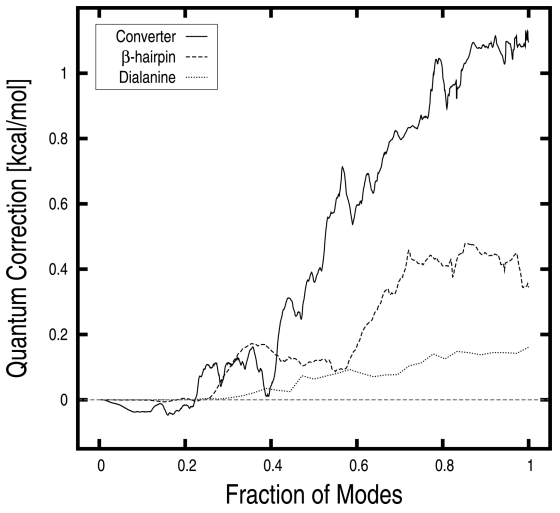

Figure 5. Room-temperature quantum corrections to the conformational ΔF for three molecular systems of increasing size: the alanine dipeptide (12 atoms), the β-hairpin of protein G (160 atoms), and the converter of myosin VI (1442 atoms). The size of the correction, which is evaluated at 300 K, is shown as a function of the fraction of normal modes included in the analysis. The modes are ranked according to their frequency in ascending order, such that the contributions from the high-frequency modes are found on the right-hand side of the plot.

that the magnitude of the correction is strongly dependent on the size of the protein with values of 0.16, 0.34, and 1.09 kcal/mol for the alanine dipeptide, the β-hairpin peptide, and the myosin converter, respectively. As discussed above, in all cases the correction arises from the zero-point energy contribution introduced by the intermediate-frequency vibrations; see Figure S5. As the number of non low-frequency modes (ν > 400 cm^{-1}) increases with the number of atoms, the size dependence of the quantum correction is not surprising. Interestingly, these results suggest a possible role for the intermediate-frequency modes on the conformational stability of biomolecules.

C. Effect of a Restraining Potential on the Quantum Correction. Efficient strategies to compute differences in conformational free energy such as umbrella sampling[55] or the confinement method[14] make use of harmonic restraints to enhance sampling of the relevant configurational space. Therefore, it is important to analyze how the quantum correction behaves in the presence of a restraining potential, which significantly perturb the vibrational frequencies of the biomolecule. For this purpose, the normal-mode frequencies of the alanine dipeptide conformers were computed in the presence of harmonic restraints of increasing magnitude; for clarity, here I used an absolute Cartesian restraint to a reference structure which had been energy minimized. Vibrational frequencies obtained at a large force constant (k of 82 kcal/mol/Å^2) are shown in Figure 2 (triangles) for illustration. The introduction of a tight harmonic restraint results in an overall increase of the vibrational frequencies, with larger changes

DOI: 10.1021/acs.jctc.5b00260
J. Chem. Theory Comput. XXXX, XXX, XXX−XXX

occurring in the low-frequency range (modes 7−17). As expected, the stronger the restraining potential (k), the higher the vibrational frequencies of the resulting modes, i.e. $\nu_i \rightarrow \infty$ as $k \rightarrow \infty$.

The values of ΔF between the **c7eq** and **c7ax** conformers calculated using quantum and classical formulas are shown in Figure 6 as a function of k. The results indicate that for k larger than 0.1 kcal/mol/Å^2 ΔF decreases monotonically with increasing k and converges to ΔU_{ff} (i.e. the potential energy difference at the minimum). Interestingly, the magnitude of the quantum correction goes to zero with increasing k; compare the separation between the black and gray circles as a function of k in Figure 6 (top). To provide with an interpretation for these observations, the frequency dependence of the enthalpic and the entropic contributions to ΔF_{vib} were analyzed. In the classical limit, the convergence of ΔF solely depends on $T\Delta S_{vib}$ (eq 7 in the SI), which goes to zero with increasing k; see Figure 6 (bottom, gray circles). By contrast, the quantum ΔF includes frequency-dependent contributions from both the zero-point energy (ΔZ_{vib}^{QM}) and the temperature-dependent vibrational energy (ΔH_{vib}^{QM}). Because ΔF_{vib}^{QM} goes as ΔZ_{vib}^{QM} in the higher-frequency range (see the Appendix), this latter determines the convergence rate of the quantum free-energy result with increasing k. Since in the presence of strong restraining forces also ΔZ_{vib}^{QM} goes to zero, i.e. at large values of k the restraining potential dominates the atomic fluctuations and the structurally diverse molecular conformers behave as nearly identical harmonic oscillators, both classical and quantum free-energy results converge to the same limit as $k \rightarrow \infty$; see Figure 6. These results support the idea that the intermediate-frequency modes, which describe partly delocalized molecular vibrations, are the only higher-frequency modes contributing to the conformational stability of biomolecules. The introduction of increasingly stronger restraints transforms the intermediate-frequency modes into more localized vibrations which become essentially independent of the molecular topology and the quantum correction vanishes.

As an aside, the results obtained for the alanine dipeptide in the presence of harmonic restraints are well behaved in the entire range, i.e. k < 3000 kcal/mol/Å^2; see Figure S6. This result indicates that the calculation of ΔF in the harmonic approximation based on quantum formulas does not diverge with increasing k, unlike previously reported.[14] The use of a restraining potential with vibration calculated with analytical second derivatives is crucial for obtaining converged free-energy results in the strong confinement (high k) range; see Figure S6 and the SI for details.

D. Quantum-Corrected Free Energy Results. The results presented above indicate that a classical treatment of protein dynamics may introduce inaccuracies in the difference of conformational free energy due to quantum effects, in particular the zero-point energy. In this context, a straightforward though approximate solution to obtain quantum-corrected free energy results from classical MD analyses may be introduced at no additional cost using the thermodynamic cycle in Figure 7. The basic idea is to link the quantum free-energy change, which is the quantity of interest, to the classical result via two unphysical transformations, which convert the actual quantum states into their classical analogs. As the difference between the free energy changes involved in the horizontal transformations can be estimated via the harmonic approximation (see equations in Figure 7), the quantum free energy change is accessed by simply adding the vibrational correction analyzed in this paper to the free-energy result obtained by classical molecular dynamics.[16] In such a scheme,

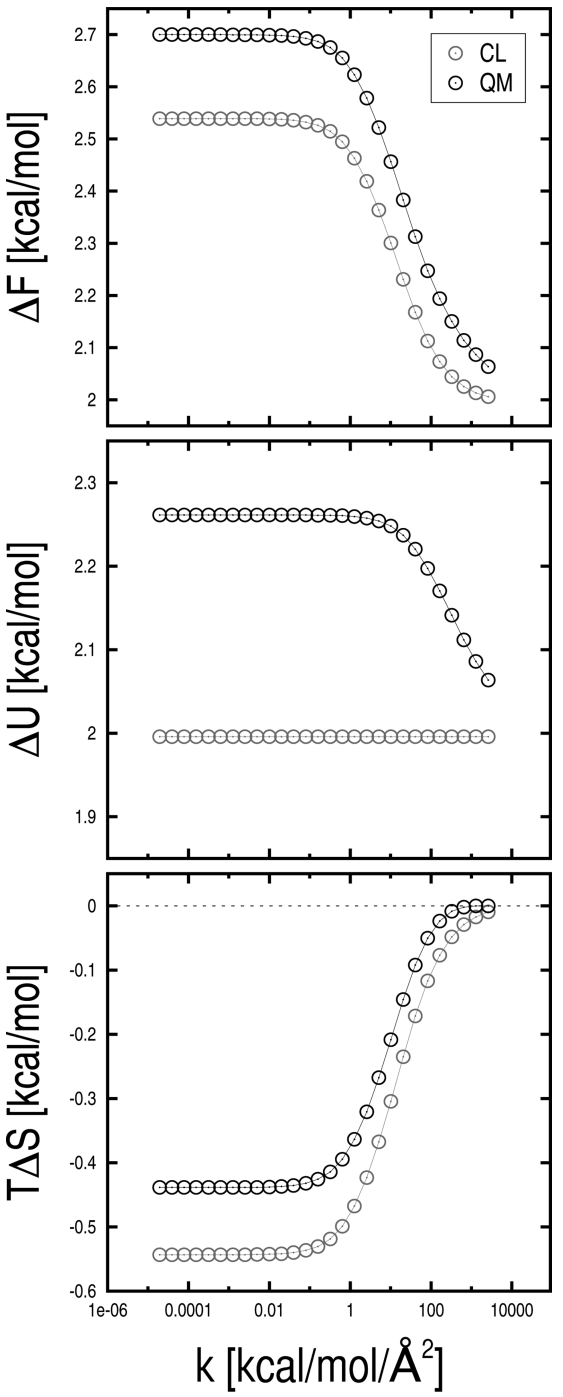

Figure 6. Analysis of the quantum corrections to ΔF, ΔU, and $T\Delta S$ for the **c7eq** and **c7ax** conformers of the alanine dipeptide in the presence of harmonic restraints of increasing strength, k. For clarity, an absolute Cartesian restraint to a reference structure, which was energy minimized beforehand, was used. Classical and quantum results are shown by gray and black circles, respectively. The Δvalues correspond to the second conformer minus the first; e.g. ΔF equals $F_{c7ax} - F_{c7eq}$. The separation between the black and the gray circles quantifies the magnitude of the quantum correction ($\Delta\Delta F$) for each value of k. The data show that the enthalpic component (ΔU) accounts for the largest contribution to the correction. However, because $\Delta\Delta U$ goes to zero with increasing k, quantum and classical free energy results converge to the same limit as $\nu \rightarrow \infty$.

DOI: 10.1021/acs.jctc.5b00260
J. Chem. Theory Comput. XXXX, XXX, XXX−XXX

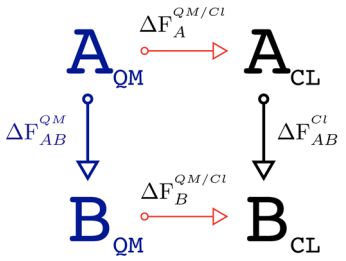

$$\Delta F_{AB}^{QM} = \Delta F_A^{QM/Cl} - \Delta F_B^{QM/Cl} + \Delta F_{AB}^{Cl}$$
$$\Delta F_A^{QM/Cl} - \Delta F_B^{QM/Cl} = \Delta F_{AB}^{QM} - \Delta F_{AB}^{Cl} = \Delta\Delta F$$

$$\Delta F_{AB}^{QM} = \Delta F_{AB}^{Cl} + \Delta\Delta F$$

Figure 7. Thermodynamic cycle describing how to include quantum corrections to the difference in free energy between the polypeptide conformers **A** and **B** obtained by classical molecular dynamics. The cycle bridges the quantum (ΔF_{AB}^{QM}) and the classical (ΔF_{AB}^{Cl}) free-energy results via two unphysical transformations that convert the actual quantum states (in blue) into their classical analogs (in black); see red arrows. By solving the thermodynamic cycle for ΔF_{AB}^{QM}, the quantum free-energy change can be expressed as a correction to the classical result via the difference between the free energy changes involved in the horizontal legs of the cycle. Here, these terms are accessed via the harmonic approximation, which provides analytical expressions for the conformational free energy both in the quantum (eq 10) and the classical (eq 14) limits. This simple though approximate approach allows one to obtain quantum-corrected free energy results from the only knowledge of the vibrational frequencies and the potential energy difference at the minimum for the two conformers.

the evaluation of the quantum correction requires only knowledge of the vibrational frequencies of the polypeptide conformers, which can be obtained by normal-mode analysis, i.e. energy minimization plus Hessian diagonalization. To illustrate the strategy, quantum-corrected free energy results for pairs of conformers of the alanine dipeptide *in vacuum* and the β-hairpin of protein G with an implicit treatment of the solvent were determined. Starting with the classical (free energy) results from previous confinement calculations,[16] quantum-corrected free energy results were obtained by using the equation given in Figure 7. Both classical and quantum-corrected free energy results are given in Table II; note that for the β-hairpin peptide the quantum correction ($\Delta\Delta F_{ho}$) was evaluated at 360 K to be consistent with the free-energy results of ref 16.

The appropriateness of the quantum-correction strategy described above was accessed by comparing in-vacuum quantum-corrected free energy results with results obtained from *ab initio* calculations in the limit of the RRHO approximation. For this benchmark, three conformers of the alanine dipeptide (c7eq, c7ax, c5) and two of tetraglycine (α, β) were considered; see the SI for the preparation of structures. These molecular systems were chosen because (i) they are sufficiently small in size that full *ab initio* calculations can be carried out efficiently and (ii) the optimized geometries in vacuum are essentially independent of the level of theory used (see the SI). To be able to compare with *ab initio* calculations, force-field results were obtained using a fully atomistic representation of the biomolecules, unlike previously done for the alanine dipeptide (see above), and with no CMAP correction, which is appropriate only in water; i.e. the param22 parametrization in CHARMM[52] was used. For the dipeptide (22 atoms), *ab initio* results were obtained at the MP2/cc-pVTZ level of theory using GAUSSIAN[56] and starting from molecular configurations that were energy-minimized at the force field level. For tetraglycine (40 atoms), because its size is double that of the dipeptide, DFT calculations based on the dispersion-corrected ωB97X-D functional[57] with the cc-pVTZ basis set were carried out. Differences in conformational free energy were then determined considering only the electronic and the vibrational contributions to the molecular partition function, which were accessed by geometry optimization in vacuum followed by a vibrational analysis of all conformers. The results are given in Table III. Assuming the quantum (MP2 or ωB97X-D) results as exact, the absolute error on ΔF can be quantified before ($\delta\Delta F$) and after ($\delta\Delta F_{corr}$) the introduction of the quantum vibrational correction analyzed here.

Table II. Quantum-Corrected Free Energy Results for the Alanine Dipeptide *in Vacuum* at 300 K and the β-Hairpin Peptide with an Implicit Treatment of the Solvent at 360 K[a]

system	states	T [K]	ΔF	$\Delta\Delta F_{ho}$	ΔF_{corr}
alanine dipeptide	**c7eq**/**c7ax**	300	2.90 ± 0.02	0.16	3.06 ± 0.02
β-hairpin peptide	**bhp1**/**bhp2**	360	1.88 ± 0.13	0.29	2.17 ± 0.13

[a]The value of ΔF corresponds to the free energy of the second conformer minus that of the first; e.g. for the alanine dipeptide ΔF equals $F_{c7ax} - F_{c7eq}$. The classical free-energy results, ΔF, were obtained from ref 16. The quantum correction, $\Delta\Delta F_{ho}$, was computed via the harmonic approximation and corresponds to $\Delta F_{ho}^{QM} - \Delta F_{ho}^{Cl}$. All free-energy values are given in kcal/mol.

On the alanine dipeptide, the free energy results obtained with the force field are in excellent agreement with those obtained at the MP2 level of theory with an absolute error of ~0.1 kcal/mol. The introduction of the quantum vibrational correction reduces the absolute error on the vibrational contribution ($\delta\Delta F_{vib}$) by 5 to 15%, although the magnitude of the correction is very small, i.e. well below 0.1 kcal/mol. Surprisingly, the quantum-corrected free energy results deviate (slightly) more from the *ab initio* results than those obtained without correction, which could indicate a spurious "double counting" of quantum effects by the *a posteriori* correction. However, the magnitude of the correction is so small (from 0.02 to 0.04 kcal/mol) that the observed deviations could also arise from the inaccuracies of the MP2/cc-pVTZ calculations, which are used as reference.

On tetraglycine, the deviation from the DFT free energy result is significantly larger (i.e., 2.68 kcal/mol), which makes it a more stringent test for the quantum vibrational correction. This time, the introduction of the correction on the ΔF between the α and β conformers decreases the absolute error by 0.64 kcal/mol (24%) and provides a more accurate estimate of the free energy change. Nonetheless, the component analysis in Table III shows that the quantum correction does not apply to the vibrational contribution, whose deviation from the quantum result actually increases when the correction is introduced, and improves the quality of the results by a cancellation of errors in the electronic contribution.

Although the present comparison is based on a rather limited data set, the results suggest that when the deviation from the

DOI: 10.1021/acs.jctc.5b00260
J. Chem. Theory Comput. XXXX, XXX, XXX−XXX

Table III. Comparison of Quantum-Corrected versus *ab Initio* Free Energy Results in the Limit of the RRHO Approximation[a]

	MP2/cc-pVTZ			param22 (no CMAP)					error	
conformers	ΔE	ΔF_{vib}	ΔF	ΔE	ΔF_{vib}^{Cl}	ΔF_{vib}^{QM}	ΔF^{Cl}	ΔF^{QM}	$\delta\Delta F$	$\delta\Delta F_{corr}$
c7eq/c7ax	2.41	−0.03	2.38	2.05	0.31	0.29	2.36	2.34	0.02	0.04
c7eq/c5	1.51	−1.26	0.25	0.92	−0.77	−0.81	0.15	0.11	0.10	0.14
c5/c7ax	0.89	1.23	2.12	1.14	1.08	1.10	2.22	2.24	0.10	0.12
	ωB97X-D/cc-pVTZ			param22 (no CMAP)					error	
conformers	ΔE	ΔF_{vib}	ΔF	ΔE	ΔF_{vib}^{Cl}	ΔF_{vib}^{QM}	ΔF^{Cl}	ΔF^{QM}	$\delta\Delta F$	$\delta\Delta F_{corr}$
α/β	11.93	−3.26	8.67	5.53	0.46	1.10	5.99	6.63	2.68	2.04

[a]Results are given for three conformers of the alanine dipeptide (c7eq, c7ax, c5) and two conformers of tetraglycine (α, β) in vacuum. The Δ values correspond to the second conformer minus the first, e.g. ΔE(c7eq/c7ax) = $E_{c7ax} - E_{c7eq}$. Taking the MP2 results as reference, $\delta\Delta F$ and $\delta\Delta F_{corr}$ quantify the absolute error before and after the inclusion of the quantum correction. For the force field results, the superscripts *Cl* and *QM* indicate calculations done using classical and quantum formulas for the vibrational partition function. The ΔE and ΔF_{vib} values correspond to the electronic and the vibrational contributions to the conformational free energy change, respectively.

quantum free energy observable is significant, the vibrational correction analyzed in this paper helps reducing the absolute error on numerical estimates based on classical analyses.

V. DISCUSSION

The results presented in this paper demonstrate that classical and quantum estimates of the free-energy difference between conformers of a biomolecule can differ by a small but not necessarily negligible amount even at room temperature. Most earlier studies that focused primarily on the vibrational entropy indicated that the low-frequency modes are dominant in the overall value. This is in accord with the fact that the mean-square fluctuations are dominated by the low-frequency modes (below 400 cm^{-1}), which are classical above 100 K. The present analysis shows that non-negligible quantum corrections at room temperature arise from the zero-point energy contribution to the vibrational energy, rather than the vibrational entropy, which is both temperature independent and linear with $h\nu$. Interestingly, the correction originates primarily from groups or bands of rather delocalized vibrations in the intermediate-frequency range, which depend on the structure of the molecule and thus may contribute to the difference in conformational free energy. In fact, their frequency is large enough to require a full quantum treatment but is sufficiently low to describe collective vibrations, in sharp contrast to the high-frequency vibrations corresponding to e.g. the stretching of the NH and OH bonds. Correspondingly, a small quantum correction to the vibrational entropy difference also arises from these intermediate-frequency nonclassical modes. Thus, the present analysis demonstrates that the high-temperature limit for the vibrational partition function, the so-called classical formula, is inappropriate for computing conformational free energy differences of biomolecules even at room temperature.

The results obtained for three biomolecular systems of variable size (i.e., from 12 to 1442 atoms) in the RRHO approximation show that the quantum correction varies from 0.2 to 1.1 kcal/mol. Although the absolute value of the calculated corrections is rather small, especially considering the inaccuracy of presently available force fields that introduce systematic deviations up to several kcal/mol dependently on the parametrization in use,[58] it is important to note that this correction is (in principle) model independent. Also, a correction of 1.1 kcal/mol, such that obtained for the converter of myosin VI, is relevant *per se* as a free-energy change of 1.4 kcal/mol corresponds to a 10-fold increase in the ligand-binding affinity for a given pharmaceutical target, which would turn a nonspecific binder into a potential candidate for lead optimization in a drug discovery project.[59] Finally, the magnitude of the quantum correction was found to correlate with the number of atoms in the system. As this correction arises from the intermediate-frequency modes, whose number increases with the size of the molecule, this finding is intriguing and suggests that sizable quantum "effects" could be involved in the structural stability of large supramolecular assemblies such as actin filaments or the virus capsid. A systematic analysis of the quantum (vibrational) correction over a larger set of proteins with variable size will provide a more definite answer on this point.

Analysis of the correction in the presence of harmonic restraints showed that the difference between quantum and classical free energy results vanishes in the limit of infinitely tight restraining potentials. Importantly, this implies that any free energy estimate obtained using harmonic restraints, i.e. umbrella sampling and confinement calculations, would differ systematically from those obtained in the absence of restraints, e.g. by long equilibrium molecular dynamics, and would be (slightly) more accurate. Similarly, free energy results obtained from independent umbrella sampling calculations making use of harmonic potentials with different strength would differ systematically because of the different magnitude of the corresponding quantum (vibrational) correction. This suggests that a systematic inclusion of the quantum correction presented in this paper would help making any comparison of free-energy results obtained with different approaches more quantitative.

More generally, the present analysis emphasizes the importance of a quantum mechanical treatment of protein dynamics for the calculation of (very) accurate conformational free-energy differences even at room temperature. The results suggest that classical molecular dynamics simulations, even when fully converged, may not be accurate enough to evaluate the thermodynamic observables, which can be accessed only through a rigorous treatment of the high-frequency vibrations. Because full *ab initio* calculations do not provide (yet) a viable solution, i.e. the computational cost required to converge on thermal averages that are strongly dependent on sampling is overwhelming even for small molecules, alternative strategies must be considered. Here, I have shown that the quantum free-energy change between conformers of a biomolecule can be estimated through a correction to the classical result via the harmonic approximation. As the correction requires only knowledge of the vibrational frequencies of the biomolecular conformers, this approach provides a straightforward though

DOI: 10.1021/acs.jctc.5b00260
J. Chem. Theory Comput. XXXX, XXX, XXX−XXX

approximate way to go beyond the limits of classical force fields and obtain *a posteriori* quantum-corrected free energy results.

One limitation of this approach concerns with the harmonic approximation itself, which neglects the contributions of the anharmonicity to the difference in free energy. Because the latter may have a substantial effect on the thermodynamics of biomolecules,[33] quasi-harmonic analyses of classical MD simulations could provide a computationally viable solution to improve the accuracy of the results. Alternatively, methods based on path integral molecular dynamics (PIMD),[60] which promise to provide direct access to the fully anharmonic quantum free-energy differences, may be invoked. Despite considerable progress in recent years,[61,62] it should be noted, however, that PIMD methods are bound to the inaccuracy of the underlying force field, which may still prevent from a "realistic" description of the role of quantum effects in proteins. Analysis of computational strategies that fully account for quantum corrections in the calculation of conformational free energy differences beyond the RRHO approximation are left for the future.

Another limitation of the quantum-correction strategy above concerns with the "effective" nature of currently available force fields for proteins, which have been empirically parametrized to reproduce inherently quantum experimental data. As such, the energy of the force field is likely to include already some quantum effects, e.g. the zero-point energy, so that any *a posteriori* inclusion of the quantum (vibrational) correction, which is *per se* correct, might lead to a spurious "double counting" and paradoxically yield results that deviate even more from the quantum observable. The analysis of the α/β conformational transition of tetraglycine in the limit of the RRHO approximation indicates that for this particular system in vacuum such "double counting" is small, and the quantum correction reduces the systematic error from the quantum (DFT) free energy change by 24%. Nonetheless, the comparison with *ab initio* free energy results in vacuum for two toy models (i.e., the alanine dipeptide and tetraglycine) indicates that the energy of the CHARMM (param22) force field does not necessarily correspond to the electronic energy of the biomolecule, such that the decomposition of the free energy into vibrational and electronic contributions would be formally incorrect even in the RRHO approximation. In this context, the use of quantum mechanically derived force fields,[63,65] which avoid the use of experimentally-derived bulk properties on purpose, would provide a more stringent theoretical framework, where the inclusion of quantum mechanical corrections like the one analyzed here, would be more meaningful.

VI. CONCLUSION

The results presented in this paper demonstrate that the intermediate-frequency vibrations ($400 < \nu < 2000$ cm^{-1}) may introduce a non-negligible contribution to the difference in free energy between conformers of a biomolecule. In particular, it is shown that they do so through the zero-point energy contribution to the vibrational energy, which emphasizes the importance of a quantum mechanical treatment of protein dynamics even at room temperature. To account for this "quantum effect", a straightforward and inexpensive strategy, that aims at the quantum reality by a vibrational correction to the classical result via the harmonic approximation, has been developed. The development of accurate and efficient quantum strategies for conformational free energy differences is a challenging but important task, which may shed light on the role of quantum effects on the conformational stability of functional biomolecules.

APPENDIX: LOW- AND HIGH-FREQUENCY LIMITS OF THE VIBRATIONAL CONTRIBUTION TO THE CONFORMATIONAL FREE-ENERGY CHANGE

I prove that the vibrational contribution to the quantum free-energy change between conformers of a biomolecule, ΔF^{QM}_{vib}, goes as the vibrational entropy change ($-T\Delta S^{QM}_{vib}$) in the low-frequency range ($\nu \ll 400$ cm^{-1}), whereas it goes as the zero-point energy difference (ΔZ^{QM}_{vib}) at higher frequencies.

In the quantum limit, the vibrational contribution to the conformational ΔF is given by

$$\Delta F^{QM}_{vib} = \Delta Z^{QM}_{vib} + \Delta H^{QM}_{vib} - T\Delta S^{QM}_{vib} \tag{A1}$$

with

$$\Delta Z^{QM}_{vib} = NkT \sum_i^{\kappa} \frac{h(\nu_i^{B} - \nu_i^{A})}{2kT} \tag{A2}$$

and

$$\Delta H^{QM}_{vib} = NkT \sum_i^{\kappa} \frac{h\nu_i^{B}/kT}{e^{h\nu_i^{B}/kT} - 1} - \frac{h\nu_i^{A}/kT}{e^{h\nu_i^{A}/kT} - 1} \tag{A3}$$

see eqs 7, 8, and 9. By setting $h\nu_i/kT = x_i$ and expanding the exponential function as a Taylor series about zero, i.e. $\exp(x) \approx 1 + x + x^2/2$, eq A3 can be rewritten as

$$\begin{aligned}\Delta H^{QM}_{vib} &= 2NkT \sum_i^{\kappa} \frac{1}{2 + x_i^{B}} - \frac{1}{2 + x_i^{A}} \\ &= 2NkT \sum_i^{\kappa} \frac{-(x_i^{B} - x_i^{A})}{(2 + x_i^{B})(2 + x_i^{A})}\end{aligned} \tag{A4}$$

which gives

$$\Delta H^{QM}_{vib} = NkT \sum_i^{\kappa} -\frac{h(\nu_i^{B} - \nu_i^{A})}{2kT} = -\Delta Z^{QM}_{vib} \tag{A5}$$

when $x_i^{B}, x_i^{A} \ll 2$, i.e. $h\nu_i \ll 2NkT$. Introducing this results into eq A1 shows that in the low-frequency range, i.e. $\nu \ll 417$ cm^{-1} at 300 K, the vibrational entropy change ($-T\Delta S^{QM}_{vib}$) is the only frequency-dependent contribution to ΔF^{QM}. In this range of frequencies, $h\nu_i \ll NkT$ and the vibrational entropy change can be safely treated using classical formulas (eq 9 in the SI). Thus, $\Delta F^{QM}_{vib} = -T\Delta S^{Cl}_{vib}$.

In the higher-frequency range, the approximations yielding the result of eq A5 do not hold. In this case, starting from eq A1 it is more useful to decompose the vibrational free-energy change as

$$\Delta F^{QM}_{vib} = \Delta Z^{QM}_{vib} + (\Delta H^{QM}_{vib} - T\Delta S^{QM}_{vib}) \tag{A6}$$

with

$$\begin{aligned}\Delta H^{QM}_{vib} - T\Delta S^{QM}_{vib} = NkT \sum_i^{\kappa} \Big[&\ln(1 - e^{-h\nu_i^{B}/kT}) \\ &- \ln(1 - e^{-h\nu_i^{A}/kT}) \Big]\end{aligned} \tag{A7}$$

and analyze the behavior of the two contributions on the r.h.s. of eq A6 with increasing ν. As $\nu \to \infty$, the first contribution (eq A2) goes as the difference between two numbers which increase linearly with ν, whereas the second contribution (eq

DOI: 10.1021/acs.jctc.5b00260
J. Chem. Theory Comput. XXXX, XXX, XXX−XXX

A7) goes to zero as the difference between two numbers that go to zero exponentially. In fact, expanding $\ln(1 - e^{-x})$ as a Taylor series about zero, i.e. $\ln(1 - e^{-x}) \approx -e^{-x} - (e^{-2x})/2$, shows that $\lim_{x\to\infty}((-e^{-x})/(\ln(1 - e^{-x}))) = 1$, which implies that $\ln(1 - e^{-x})$ goes to zero exponentially as $x \to \infty$. Thus, the second contribution of eq A6 vanishes very rapidly with increasing ν, and $\Delta Z_{\mathrm{vib}}^{QM}$ is the only frequency-dependent contribution to ΔF^{QM} in the higher-frequency range, i.e. $\nu > 400\ \mathrm{cm}^{-1}$.

■ ASSOCIATED CONTENT

Supporting Information

The Supporting Information is available free of charge on the ACS Publications website at DOI: 10.1021/acs.jctc.5b00260.

Analysis of the interplay between energy and entropy contributions to the vibrational free energy in frequency and temperature; a formal derivation of the vibrational partition function in both quantum and classical limits; a deconvolution of the quantum correction in enthalpic and entropic contributions; a discussion on the divergence of the quantum vibrational free energy in the presence of large restraining forces; details on the preparation of structures for the comparison with *ab initio* free-energy results; the vibrational frequencies of the alanine dipeptide; vibrational analyses of the β-hairpin and the converter of myosin VI (PDF)

■ AUTHOR INFORMATION

Corresponding Author

*E-mail: mcecchini@unistra.fr.

Notes

The authors declare no competing financial interest.

■ ACKNOWLEDGMENTS

I am most indebted to Martin Karplus for invaluable mentoring over these years. His critical reading of the manuscript is gratefully acknowledged. Also, I would like to thank Guido Pupillo and Roberto Marquardt for useful discussions and Simone Conti for running all *ab initio* calculations. The research was supported by the Agence Nationale de la Recherche through the LabEx project Chemistry of Complex Systems (ANR-10-LABX-0026_CSC) and the International Center for Frontier Research in Chemistry (icFRC). The work was granted access to the HPC resources of [CCRT/CINES/IDRIS] under the allocation 2014-[076644] made by GENCI (Grand Equipement National de Calcul Intensif).

■ REFERENCES

(1) Makhatadze, G. I.; Privalov, P. L. Energetics of protein structure. *Adv. Protein Chem.* **1995**, *47*, 307−425.

(2) Karplus, M. Behind the folding funnel diagram. *Nat. Chem. Biol.* **2011**, *7*, 401−404.

(3) McQuarrie, D. *Statistical Mechanics*; Harper and Row: New York, 1976.

(4) Frenkel, D.; Smit, B. *Understanding molecular simulation: from algorithms to applications*; Academic Press: 2001; Vol. *1*.

(5) Meirovitch, H. Recent developments in methodologies for calculating the entropy and free energy of biological systems by computer simulation. *Curr. Opin. Struct. Biol.* **2007**, *17*, 181−186.

(6) Kirkwood, J. Statistical mechanics of fluid mixtures. *J. Chem. Phys.* **1935**, *3*, 300.

(7) Zwanzig, R. High-temperature equation of state by a perturbation method. I. Nonpolar gases. *J. Chem. Phys.* **1954**, *22*, 1420−1426.

(8) Tembre, B.; Mc Cammon, J. Ligand-receptor interactions. *Comput. Chem. (Oxford, U. K.)* **1984**, *8*, 281−283.

(9) Gao, J.; Kuczera, K.; Tidor, B.; Karplus, M. Hidden thermodynamics of mutant proteins: A molecular dynamics analysis. *Science* **1989**, *244*, 1069.

(10) Archontis, G.; Simonson, T.; Karplus, M. Binding free energies and free energy components from molecular dynamics and Poisson-Boltzmann calculations. Application to amino acid recognition by aspartyl-tRNA synthetase1. *J. Mol. Biol.* **2001**, *306*, 307−327.

(11) Shirts, M.; Pitera, J.; Swope, W.; Pande, V. Extremely precise free energy calculations of amino acid side chain analogs: Comparison of common molecular mechanics force fields for proteins. *J. Chem. Phys.* **2003**, *119*, 5740.

(12) Elber, R. Long-timescale simulation methods. *Curr. Opin. Struct. Biol.* **2005**, *15*, 151−156.

(13) Zuckerman, D. Equilibrium sampling in biomolecular simulations. *Annu. Rev. Biophys.* **2011**, *40*, 41−62.

(14) Tyka, M.; Clarke, A.; Sessions, R. An efficient, path-independent method for free-energy calculations. *J. Phys. Chem. B* **2006**, *110*, 17212−17220.

(15) Park, S.; Lau, A.; Roux, B. Computing conformational free energy by deactivated morphing. *J. Chem. Phys.* **2008**, *129*, 134102.

(16) Cecchini, M.; Krivov, S.; Spichty, M.; Karplus, M. Calculation of Free-Energy Differences by Confinement Simulations. Application to Peptide Conformers. *J. Phys. Chem. B* **2009**, *113*, 9728−9740.

(17) Hensen, U.; Lange, O.; Grubmüller, H.; Langowski, J. Estimating Absolute Configurational Entropies of Macromolecules: The Minimally Coupled Subspace Approach. *PLoS One* **2010**, *5*, e9179.

(18) Ovchinnikov, V.; Cecchini, M.; Karplus, M. A Simplified Confinement Method (SCM) for Calculating Absolute Free Energies and Free Energy and Entropy Differences. *J. Phys. Chem. B* **2013**, *117*, 750−762.

(19) Esque, J.; Cecchini, M. Accurate Calculation of Conformational Free Energy Differences in Explicit Water: The Confinement-Solvation Free Energy Approach. *J. Phys. Chem. B* **2015**, *119*, 5194−5207.

(20) Ovchinnikov, V.; Karplus, M.; Vanden-Eijnden, E. Free energy of conformational transition paths in biomolecules: The string method and its application to myosin VI. *J. Chem. Phys.* **2011**, *134*, 085103.

(21) Maragakis, P.; Spichty, M.; Karplus, M. A Differential Fluctuation Theorem. *J. Phys. Chem. B* **2008**, *112*, 6168−6174.

(22) Spichty, M.; Cecchini, M.; Karplus, M. Conformational Free-Energy Difference of a Miniprotein from Nonequilibrium Simulations. *J. Phys. Chem. Lett.* **2010**, *1*, 1922−1926.

(23) Karplus, M.; Kushick, J. Method for estimating the configurational entropy of macromolecules. *Macromolecules* **1981**, *14*, 325−332.

(24) Brooks, B.; Karplus, M. Harmonic dynamics of proteins: normal modes and fluctuations in bovine pancreatic trypsin inhibitor. *Proc. Natl. Acad. Sci. U. S. A.* **1983**, *80*, 6571.

(25) Tidor, B.; Karplus, M. The Contribution of Vibrational Entropy to Molecular Association: The Dimerization of Insulin. *J. Mol. Biol.* **1994**, *238*, 405−414.

(26) Levy, R.; Perahia, D.; Karplus, M. Molecular dynamics of an α-helical polypeptide: Temperature dependence and deviation from harmonic behavior. *Proc. Natl. Acad. Sci. U. S. A.* **1982**, *79*, 1346.

(27) Wong, C.; Zheng, C.; Shen, J.; McCammon, J.; Wolynes, P. Cytochrome C: a molecular proving ground for computer simulations. *J. Phys. Chem.* **1993**, *97*, 3100−3110.

(28) Roitberg, A.; Gerber, R.; Ratner, M. A Vibrational Eigenfunction of a Protein: Anharmonic Coupled-Mode Ground and Fundamental Excited States of BPTI. *J. Phys. Chem. B* **1997**, *101*, 1700−1706.

(29) Garcia-Viloca, M.; Gao, J.; Karplus, M.; Truhlar, D. How enzymes work: Analysis by modern rate theory and computer simulations. *Science* **2004**, *303*, 186.

(30) Wong, K.; Sonnenberg, J.; Paesani, F.; Yamamoto, T.; Vaníček, J.; Zhang, W.; Schlegel, H.; Case, D.; Cheatham, T., III; Miller, W.; et al. Proton transfer studied using a combined ab initio reactive

DOI: 10.1021/acs.jctc.5b00260
J. Chem. Theory Comput. XXXX, XXX, XXX−XXX

potential energy surface with quantum path integral methodology. *J. Chem. Theory Comput.* **2010**, *6*, 2566.
(31) Liu, J.; Miller, W.; Paesani, F.; Zhang, W.; Case, D. Quantum dynamical effects in liquid water: A semiclassical study on the diffusion and the infrared absorption spectrum. *J. Chem. Phys.* **2009**, *131*, 164509.
(32) Schreiner, P.; Reisenauer, H.; Ley, D.; Gerbig, D.; Wu, C.; Allen, W. Methylhydroxycarbene: Tunneling Control of a Chemical Reaction. *Science* **2011**, *332*, 1300.
(33) Levy, R.; Karplus, M.; Kushick, J.; Perahia, D. Evaluation of the configurational entropy for proteins: application to molecular dynamics simulations of an α-helix. *Macromolecules* **1984**, *17*, 1370−1374.
(34) Schlitter, J. Estimation of absolute and relative entropies of macromolecules using the covariance matrix. *Chem. Phys. Lett.* **1993**, *215*, 617−621.
(35) Andricioaei, I.; Karplus, M. On the calculation of entropy from covariance matrices of the atomic fluctuations. *J. Chem. Phys.* **2001**, *115*, 6289.
(36) Friesner, R.; Levy, R. An optimized harmonic reference system for the evaluation of discretized path integrals. *J. Chem. Phys.* **1984**, *80*, 4488.
(37) Andricioaei, I.; Straub, J. E.; Karplus, M. Simulation of quantum systems using path integrals in a generalized ensemble. *Chem. Phys. Lett.* **2001**, *346*, 274−282.
(38) Brooks, B.; Bruccoleri, R.; Olafson, B.; States, D.; Swaminathan, S.; Karplus, M. CHARMM: a program for macromolecular energy, minimization, and dynamics calculations. *J. Comput. Chem.* **1983**, *4*, 187−217.
(39) Brooks, B. R.; Brooks, C. L.; MacKerell, A. D.; Nilsson, L.; Petrella, R. J.; Roux, B.; Won, Y.; Archontis, G.; Bartels, C.; Boresch, S.; et al. CHARMM: the biomolecular simulation program. *J. Comput. Chem.* **2009**, *30*, 1545−1614.
(40) Olender, R.; Elber, R. Calculation of classical trajectories with a very large time step: Formalism and numerical examples. *J. Chem. Phys.* **1996**, *105*, 9299.
(41) Smith, P. The alanine dipeptide free energy surface in solution. *J. Chem. Phys.* **1999**, *111*, 5568.
(42) Ren, W.; Vanden-Eijnden, E.; Maragakis, P.; Weinan, E. Transition pathways in complex systems: Application of the finite-temperature string method to the alanine dipeptide. *J. Chem. Phys.* **2005**, *123*, 134109.
(43) van der Vaart, A.; Karplus, M. Simulation of conformational transitions by the restricted perturbation-targeted molecular dynamics method. *J. Chem. Phys.* **2005**, *122*, 114903.
(44) Neria, E.; Fischer, S.; Karplus, M. Simulation of activation free energies in molecular systems. *J. Chem. Phys.* **1996**, *105*, 1902−1921.
(45) Gronenborn, A.; Filpula, D.; Essig, N.; Achari, A.; Whitlow, M.; Wingfield, P.; Clore, G. A novel, highly stable fold of the immunoglobulin binding domain of streptococcal protein G. *Science* **1991**, *253*, 657−661.
(46) Krivov, S.; Karplus, M. Hidden complexity of free energy surfaces for peptide (protein) folding. *Proc. Natl. Acad. Sci. U. S. A.* **2004**, *101*, 14766.
(47) Lazaridis, T.; Karplus, M. Effective Energy Function for Proteins in Solution. *Proteins: Struct., Funct., Genet.* **1999**, *35*, 133−152.
(48) Geeves, M.; Holmes, K. Structural mechanism of muscle contraction. *Annu. Rev. Biochem.* **1999**, *68*, 687−728.
(49) Ménétrey, J.; Llinas, P.; Mukherjea, M.; Sweeney, H.; Houdusse, A. The structural basis for the large powerstroke of myosin VI. *Cell* **2007**, *131*, 300−308.
(50) Rock, R.; Ramamurthy, B.; Dunn, A.; Beccafico, S.; Rami, B.; Morris, C.; Spink, B.; Franzini-Armstrong, C.; Spudich, J.; Sweeney, H. A flexible domain is essential for the large step size and processivity of myosin VI. *Mol. Cell* **2005**, *17*, 603−609.
(51) Ovchinnikov, V.; Cecchini, M.; Vanden-Eijnden, E.; Karplus, M. A Conformational Transition in the Myosin VI Converter Contributes to the Variable Step Size. *Biophys. J.* **2011**, *101*, 2436−2444.
(52) MacKerell, A. D., Jr.; Bashford, D.; Bellott, M.; Dunbrack, R., Jr; Evanseck, J.; Field, M.; Fischer, S.; Gao, J.; Guo, H.; Ha, S.; et al. All-atom empirical potential for molecular modeling and dynamics studies of proteins. *J. Phys. Chem. B* **1998**, *102*, 3586−3616.
(53) Mackerell, A., Jr; Feig, M.; Brooks, C., III Extending the treatment of backbone energetics in protein force fields: limitations of gas-phase quantum mechanics in reproducing protein conformational distributions in molecular dynamics simulations. *J. Comput. Chem.* **2004**, *25*, 1400−1415.
(54) Haberthür, U.; Caflisch, A. FACTS: Fast analytical continuum treatment of solvation. *J. Comput. Chem.* **2008**, *29*, 701−715.
(55) Torrie, G.; Valleau, J. Nonphysical sampling distributions in Monte Carlo free-energy estimation: Umbrella sampling. *J. Comput. Phys.* **1977**, *23*, 187−199.
(56) Frisch, M. J. et al. *Gaussian 09 Revision A.02*; Gaussian Inc.: Wallingford, CT, 2009.
(57) Chai, J.-D.; Head-Gordon, M. Long-range corrected hybrid density functionals with damped atom-atom dispersion corrections. *Phys. Chem. Chem. Phys.* **2008**, *10*, 6615−6620.
(58) Beauchamp, K. A.; Lin, Y.-S.; Das, R.; Pande, V. S. Are protein force fields getting better? A systematic benchmark on 524 diverse NMR measurements. *J. Chem. Theory Comput.* **2012**, *8*, 1409−1414.
(59) Hopkins, A.; Groom, C.; Alex, A. Ligand efficiency: a useful metric for lead selection. *Drug Discovery Today* **2004**, *9*, 430−431.
(60) Craig, I. R.; Manolopoulos, D. E. Quantum statistics and classical mechanics: Real time correlation functions from ring polymer molecular dynamics. *J. Chem. Phys.* **2004**, *121*, 3368−3373.
(61) Ceriotti, M.; Parrinello, M.; Markland, T. E.; Manolopoulos, D. E. Efficient stochastic thermostatting of path integral molecular dynamics. *J. Chem. Phys.* **2010**, *133*, 124104.
(62) Peng, Y.; Cao, Z.; Zhou, R.; Voth, G. A. Path Integral Coarse-Graining Replica Exchange Method for Enhanced Sampling. *J. Chem. Theory Comput.* **2014**, *10*, 3634−3640.
(63) Grimme, S. A general quantum mechanically derived force field (QMDFF) for molecules and condensed phase simulations. *J. Chem. Theory Comput.* **2014**, *10*, 4497−4514.
(64) DeLano, W. L. *PyMOL Molecular Graphics System*, 2002. https://www.pymol.org// (accessed July 30, 2015).
(65) Giese, T. J.; et al. Recent advances toward a general purpose linear-scaling quantum force field. *Acc. Chem. Res.* **2014**, *47*, 2812−2820.

NOTE ADDED AFTER ASAP PUBLICATION

This article was published ASAP on August 18, 2015. A correction has been made to equation 11. The correct version was reposted on August 18, 2015.

DOI: 10.1021/acs.jctc.5b00260
J. Chem. Theory Comput. XXXX, XXX, XXX−XXX